Review of Two Retarding Potential Analyzers for Use in High Density Helicon Plasma

IEPC-2007-161

Presented at the 30th International Electric Propulsion Conference, Florence, Italy
September 17-20, 2007

Kristina M. Lemmer,[1] Alec D. Gallimore,[2] Timothy B. Smith[3] and Daniel R. Austin[4]
University of Michigan, Ann Arbor, MI, 48109, USA

Abstract: Retarding Potential Analyzers (RPAs) are compact, inexpensive diagnostics capable of measuring ion energy distribution functions (IEDFs) by using, traditionally, a series of grids to selectively filter ions of differing potentials. Two RPAs have been built, calibrated using the monoenergetic ion beam of a 3-cm-diameter gridded ion source, and tested in the discharge of a 15-cm-diameter helicon source at the University of Michigan Plasmadynamics and Electric Propulsion Laboratory (PEPL). The first RPA (Micro RPA or MRPA) is a small, compact gridded design developed at Australia National University in Canberra specifically for helicon plasma measurements. The second RPA (Slit RPA or SRPA) is a new PEPL design that substitutes adjustable-width slits for the traditional constant-diameter grid apertures, facilitating the matching of slit width to the ion Debye length for high-density plasmas. We found that measurements in the beam of a 3-cm-diameter ion source gave similar results for both analyzers. Ion energy distribution functions (IEDFs) measured on the helicon source differed greatly between the two RPAs. Results from the SRPA show ion energies about 2 to 3 times that measured by the MRPA. The MRPA measured ion energies between 17 V and 40 V, where as the SRPA measured ion energies between 55 V and 100 V. Possible explanations for the differences are explored.

Nomenclature

A_c	=	collector area
I	=	ion current
k_b	=	Boltzmann's constant
m_i	=	ion mass
n_e	=	electron number density
n_i	=	ion number density
q_e	=	elementary charge
T_e	=	electron temperature
V	=	retarding potential
V_d	=	potential difference between grids

[1] Graduate Student Research Assistant, Aerospace Engineering, klemmer@umich.edu.
[2] Arthur F. Thurnau Professor of Aerospace Engineering and Applied Physics, Associate Dean for Academic Programs and Initiatives, Rackham Graduate School, alec.gallimore@umich.edu
[3] Research Fellow, Aerospace Engineering, and timsmith@umich.edu.
[4] Student, Aerospace Engineering, and danausti@umich.edu.

V_{mp} = most probable ion voltage
V_r = electron-repelling potential
V_s = electron-suppressing potential
x = grid spacing
Z_i = ith charge state
ε_o = permittivity of free space
λ_D = Debye Length

I. Introduction

HELICON sources are highly efficient RF plasma sources capable of producing plasma densities as high as ~10^{20} m^{-3} with electron temperatures only around 3 eV. For this reason, there is much interest in using helicon sources in all aspects of plasmadynamic research from plasma processing to electric propulsion. At the University of Michigan Plasmadynamics and Electric Propulsion Laboratory (PEPL) we have developed a 15-cm-diameter helicon source for a variety of purposes. These include simulating atmospheric re-entry plasma conditions in a laboratory setting and researching the feasibility of using a helicon as an ionization source for a Hall effect thruster (HET).

During atmospheric re-entry, capsules become surrounded by high density, low temperature plasma. Densities of around 10^{16} – 10^{19} m^{-3} and electron temperatures around 2 – 5 eV have been measured during the re-entry of a RAM-C capsule in the 1960's.[1,2] The densities and electron temperatures downstream of the PEPL helicon source match well with the lower densities (higher altitudes) and electron temperatures found in the RAM-C experiments. In addition to the ion number density and the electron temperature, we are interested in measuring the ion energy downstream of the helicon source. This is measured using a retarding potential analyzer (RPA).[3]

Modern spacecraft are increasingly using electric propulsion devices for station keeping and orbit topping maneuvers. HETs are used most often for near earth maneuvers, such as those mentioned above, due to their high specific impulse and reasonable electrical efficiency. However, the reliance of HETs on DC electron bombardment for gas ionization limits the thrust efficiency as well as the range of specific impulses.[4] Helicons, known as the *most efficient method for producing high density, low temperature plasma,*[5] may be able to alleviate some of the issues that arise from using DC cathodes as the main source of ionization in HETs. In order to determine the feasibility of using helicon sources on HETs, we must first determine whether the plasma is exiting the helicon at a sufficient rate for the HET. Again, this is determined through the use of a RPA.

The RPA is a diagnostic that collects selectively filtered ions via the application of a varying grid potential. Thus, only ions with energy to charge ratios (E/q) greater than the grid voltage can pass through the grid apertures to reach the collector. The magnitude of the derivative of the resulting current vs. voltage curve is proportional to the ion energy distribution[3].

In this study, we developed and tested two RPAs for use on the PEPL helicon source. We built one RPA (the micro RPA or MRPA) based on a design used at Australia National University in Canberra by Conway et al. specifically for use with helicon sources.[6] The second RPA is a new PEPL design that substitutes adjustable-width slits for the traditional constant-diameter grid apertures,[5] facilitating the matching of slit width to the ion Debye length for high-density plasmas. This allows for more versatility when operating in plasmas of various densities, as is common at PEPL. Both RPAs were calibrated using the monoenergetic ion beam of a 3-cm-diameter gridded calibration source that provided a constant beam voltage at 300V. After calibration, we placed the RPAs in the discharge of the PEPL 15-cm-diameter helicon source. Ion energy distribution functions (IEDFs) were calculated from the current vs. voltage characteristics and compared for the two RPAs. We present these results in this paper.

II. Design Considerations

When designing an RPA, the first consideration is the spacing between the electron repelling and the ion retarding grids with respect to space-charge limitations.[3] This occurs when, as positively or negatively charged species are removed from the flow, additional charge builds up between the grids, creating a potential hill. If this potential hill increases to the point where it is greater than the applied voltage, then the operation of the RPA will change. This results in a lowering of the collected current of that species. The relationship between the grid spacing, x, and the potential difference between the grids, V_d, is given in Eq. (1) for the case when any higher plasma density would lead to space-charge limitations.

[5] Conversations between Timothy B. Smith and Kristina M. Lemmer, University of Michigan, October 2006.

$$x/\lambda_D = 1.02\left(q_e V_d / k_b T_e\right)^{3/4} \tag{1}$$

$$\lambda_D = \sqrt{\left[\left(\varepsilon_o k_b T_e\right)/\left(n_e q_e^2\right)\right]} \tag{2}$$

Equation 2 is an expression to determine the Debye length, where λ_D is the Debye length, q_e is the charge of an electron, k_b is Boltzmann's constant, T_e is the electron temperature in Kelvin, ε_o is the permittivity of free space, and n_e is the plasma electron density. Since V_d is generally set to a few times T_e (to ensure that all electrons are repelled), the spacing between the ion-retarding grid and the electron-repelling grid should be set to satisfy the condition in Eq. (3).

$$x < 4\lambda_D \tag{3}$$

In the case of the PEPL helicon plasma source, where the plasma density is on the order of 10^{18} m^{-3}, this requires a grid spacing of less than 0.1 mm. For our experiments we are taking RPA measurements downstream of the helicon discharge where densities are closer to 10^{17} m^{-3}. This requires grid spacing less than 0.5 mm, which is difficult to build in the lab. To circumvent this issue, we place floating attenuation grids on the front of the analyzer to lower the plasma density entering the RPA.

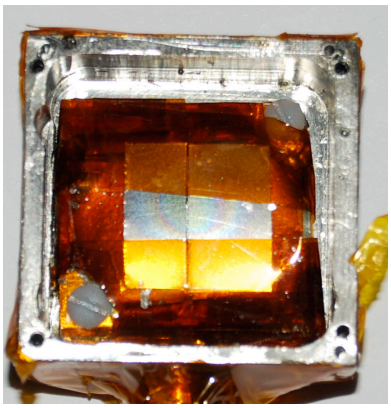

Figure 1. Slits in the SRPA design

Another design consideration that we looked at was the size of the grid aperture. In order for the grids to be effective, the diameter of the grid aperture must be much less than the Debye length, while still maintaining a high signal to noise ratio. This design consideration led us a different type of RPA design, which does not have fixed diameter grids as the filters since this type of RPA is designed to work with a narrow range of plasma densities. If we were to stray outside that range, either the grids would not work as effective filters, instead creating a potential valley through which the particles accelerate (for higher densities), or the grids would block too many of the ions, resulting in a signal to noise ratio that is unacceptable (for lower densities).

Since we use many types of plasma devices at PEPL, we wanted to design a RPA that can operate in different ranges of plasma densities. Thus, we decided upon a slit design that allows for a degree of freedom in the gap thickness. Therefore, when we want to operate the RPA in low-density plasma, we can increase the gap, and when we want to operate the analyzer in high-density plasma, we can narrow it. Figure 1 is a photo of the slit inside of the SRPA. Although the intention of the SRPA is for the slit width to be adjustable, for our initial attempt, we chose to fix the gap width to simplify the construction.

III. Facilities and Experimental Setup

A. Facilities

All testing was performed at PEPL at the University of Michigan in the Cathode Test Facility (CTF). The CTF is a 2.44-m-long by 0.61-m-diameter aluminum vacuum chamber. There is a CVI TM500 cryopump with a measured xenon pumping speed of 1,500 l/s attached to the CTF that is able to pump down to a base pressure of ~3 E-7 Torr and able to maintain pressures up to ~10 E -3 Torr without overheating. The helicon is attached to a 14.5-cm-diameter port that is located on the side of the CTF. In addition, there is one high precision linear table with attached external motion controller that allows for variations in the axial direction during diagnostics testing. A five-panel graphite beam dump protects the cryopump and prevents back sputtering caused by an ion beam.

B. 3-cm-Diameter Ion Source Setup

For calibration of the RPAs, we used a Commonwealth Scientific 3-cm-diameter gridded ion source, shown in Fig. Figure 2. This unit is capable of operation up to 1,500 V; however, we only ran the system at 300 V. The ion source consists of an outer body made of 1.6 mm thick stainless steel. There are two grids, screen and accelerator,

that are 1 mm thick discs with a laser-drilled hexagonal pattern of holes with 1-mm-diameter apertures and 1.32-mm-spacing between aperture centers. A needle valve was used to constrict xenon flow so that we could maintain a constant chamber pressure of ~8.5 E-5 Torr. A Kikisui PAD 16-10L supplies power to the 0.25-mm-diameter tungsten cathode filament, while a Hewlett Packard HP 6271 maintains the discharge current and voltage. Both of these power supplies float atop a Glassman FC01.5P80 1500 V, 80 mA power supply that provides the beam potential. Power to the accelerator grid is provided by a Lambda model 71 supply, and a 10-ampere Variac powers the neutralizer wire.

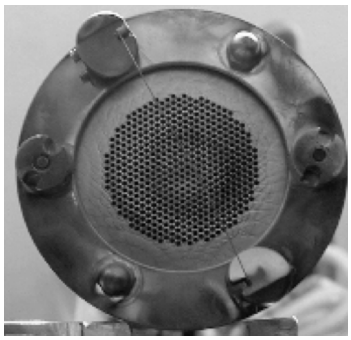

Figure 2. 3 cm gridded ion source.

C. Helicon Setup

The helicon source at PEPL has a double helix antenna (Fig. 3a) wrapped around a 15-cm-diameter by 40-cm-long quartz tube and connected via a pi-style matching network to a 3 kW, 13.56 MHz RF power supply. The matching network allows for peak reflected power in the range of 10 – 50 watts for the majority of the operating conditions. There are also three magnets capable of creating a peak magnetic field of 415 gauss along the helicon centerline. We flow argon into the CTF via a needle valve at about

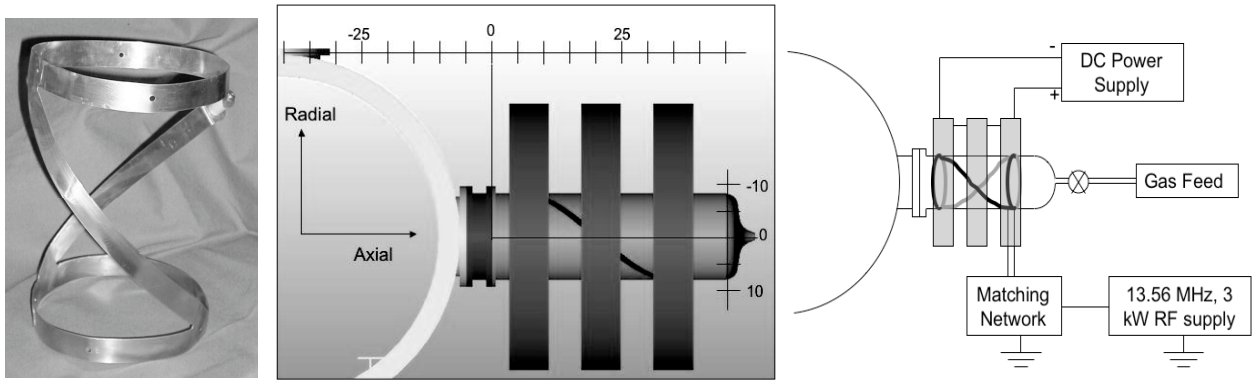

a) b) c)

Figure 3. PEPL helicon source setup. *a) Double helix antenna. b) Helicon source layout with dimensions. Units are in cm. The (0,0) location is where the quartz tube meets the CTF flange in the radial center of the quartz tube. The magnets and antenna are seen surrounding the quartz tube. c) Helicon electrical setup showing DC magnets, RF antenna, pi-style matching network and RF power supply.*

~200 sccm through an inlet nozzle at the end of the quartz tube. This creates a background pressure of between 0.9 and 1.1 mTorr. Fig. 3Figure 3b shows the layout of the PEPL helicon source, and Fig. 3Figure 3c shows the electrical setup of the helicon.

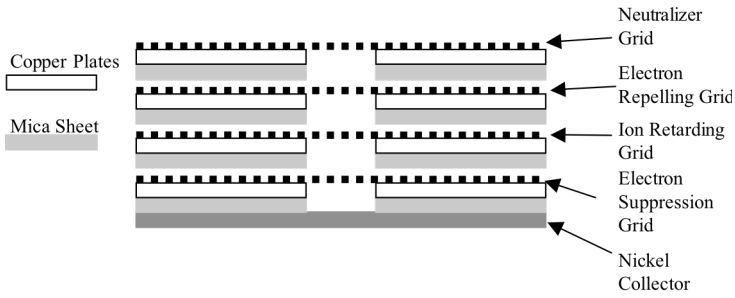

Figure 4. Schematic of MRPA. *Four grid design with mica sheet for spacers. The grids are in physical contact with copper plates in order to create electrical contacts.*

D. Retarding Potential Analyzers

1. Micro Retarding Potential Analyzer

We designed the MRPA based on both the multi-grid energy analyzer design recommended by Hutchinson[3] and a design previously used at the Australia National University in Canberra.[6] Figure 4 shows a schematic of our 4-grid design, and Fig. 5 is a photo of the MRPA.

The analyzer is housed inside a stainless steel case that is 21 mm x 13.75 mm x 26.5 mm, and a 9.75-mm-diameter stainless steel tube encloses the electrical connections for the grids. The housing lid

has two sides, creating a partial box, ensuring that the only ions entering the analyzer are those entering through the front orifice. The plasma first passes through an attenuating grid that is floating on the outside of the MRPA. Next, it passes into the analyzer and then through the floating neutralizer grid, negatively charged electron-repelling grid, positively charged and varying ion-retarding grid, and finally through the negatively charged electron-suppression grid. If the ion passes through all these filters, it then collides with a nickel collector plate. Each grid consists of a stainless steel mesh with 0.28-mm-diameter grid apertures, a copper plate that provides a means of charging the mesh and a mica sheet for insulation. The resulting space between grids is 0.71 mm. This is slightly higher than four times the expected Debye length (0.3 mm), so a series of attenuating grids have been added to the front of the MRPA in order to lower the density inside the analyzer. The grid assembly is stacked inside of and clamped to the housing lid, which is then bolted to the remainder of the housing.

A varying voltage from 0 V to 500 V is applied to the ion-retarding grid via a Keithley 2410 source meter. We use batteries to put a constant 0 V to -11.3 V potential on the electron-suppression grid and a constant 0 V to -100 V potential on the electron-retarding grid. Current collected from the nickel plate is measured via a Keithley 6485 picoammeter.

2. Slit Retarding Potential Analyzer

As stated earlier, we chose the design of the SRPA to allow for changing the slit width depending on the density of the plasma within which the analyzer will be operated. Due to our desire to create a simple design for the first time that we operated the SRPA, however, we chose to fix the slit width on this version. We designed the analyzer such that the slit width is equal to the diameter of the grid apertures in the mesh used in the MRPA. In addition, we placed a stainless steel mesh at the entrance to the analyzer to lower the plasma density inside the SRPA. Figure 5 shows the two RPAs side-by-side.

Figure 5. MRPA on the right and SRPA on the left.

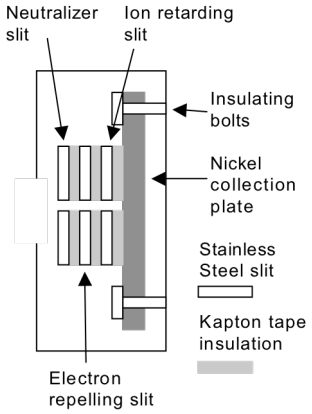

Figure 6. Schematic drawing of SRPA

The SRPA consists of three stainless steel framed slits that the plasma must pass through before reaching a nickel collector plate. The first slit is the neutralizer slit, the second is the electron-repelling slit, and the third is the ion-retarding slit. We chose not to include an electron-suppression slit in the initial version of the SRPA to make the design as simple as possible. Layers of kapton tape for insulation separate the slits. This results in a slit separation distance of .72 mm, very close to that of the MRPA. In the future, we plan to add an electron-suppression grid and to make the slit width adjustable. Figure 6 is a schematic of the SRPA.

Similar to the MRPA, a varying voltage from 0 V to 500 V was applied to the ion retarding slit using a Keithley 2410. We again used batteries to provide the constant negative potential on the electron-repelling slit ranging from 0 V to -100 V, and we used a Keithley 6485 picoammeter to measure the current collected by the nickel plate.

IV. Data Analysis and Results

The collector current and discriminator voltage are recorded by a PC using a LabVIEW code. Then, we smooth the data using a 7-point-box smoothing spline before and after numerically differentiating the current vs. voltage characteristic to reduce the effects of noise on the measured signal. From Eq. (4) we know that dI/dV is proportional to the IEDF.

$$\frac{dI}{dV} = -\frac{q_e^2 Z_i^2 n_i A_c}{m_i} f(V) \propto -f(V) \tag{4}$$

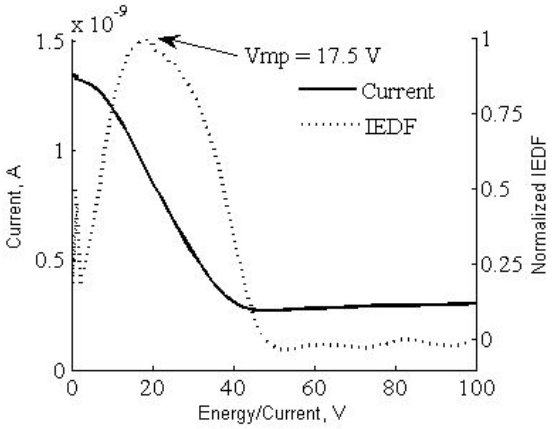

Figure 7. Example of data analysis process. *Sweep taken with MRPA with V_r=-60 V and V_s=-11.3 V. Helicon power set to 500 W.*

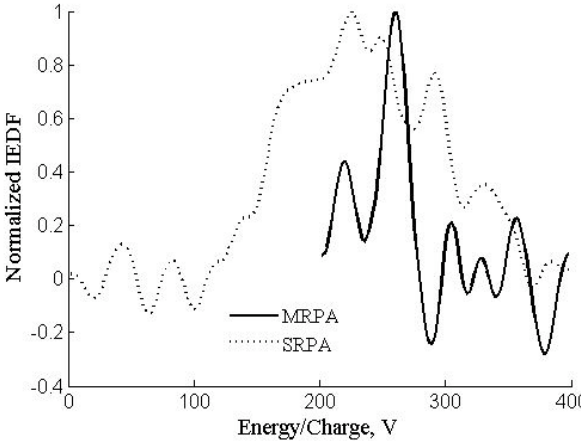

Figure 8. Normalized IEDF as a function of Energy/Charge. *Most probable ion energy occurs at peak of dI/dV plot. V_r = -60 V, V_s = -5.7 V.*

In the equation above, Z_i is the charge state of the ions, n_i is the ion number density, A_c is the area of the collector, and m_i is the mass of an ion. The IEDFs are normalized to a peak of 1 in order to facilitate comparing of characteristics. The potential where the peak dI/dV occurs in the IEDF indicates the most probable ion voltage, V_{mp}. Figure 7 shows an example current vs. voltage sweep, as well its IEDF.

A. Calibration Using Ion Source

Before testing the RPAs in the discharge of a helicon source, we wanted to make sure that they were operating as we expected. By using the Commonweath Scientific 3-cm-diameter ion source, we were able to set a known ion energy equal to the difference between the beam voltage, V_b and the plasma potential. The analyzer was located 25 cm downstream and along the centerline of the ion source, while the ion source was operating at a 300 V beam potential. We measured the most probably ion potential to be approximately 250 V. Figure 8 shows plots of the IEDFs from each RPA. The peak, though wide, is nevertheless located around 250 V. One possible reason for the lower than expected ion potential (300 V) is because we did not use thoriated tungsten as the neutralizer wire thus, limiting its ability to neutralize the plasma. Therefore, the plasma potential may have been higher than the expected value of around 0 V.[7] The wide peak and fluctuating signal are due to low density downstream of the ion source. Since both RPAs were designed for operation in the high-density plume of a helicon source, very little current actually passes through all the grids to hit the nickel current collector (less than nanoamperes), resulting in a low signal to noise ratio. This situation is a great example of where a RPA with an adjustable width slit instead of fixed grids would be most useful.

B. Helicon Testing Results

One difficulty that arose during testing was the low current being collected by the analyzers. We expected to collect currents in the microampere range;[6,8] however, we were collecting nanoamperes. This is because the density in which we operated the analyzers was lower than what we expected. Since we expected to operate the analyzers within plasma densities of 10^{17} m^{-3}, and we were actually operating within plasma densities of 10^{16} m^{-3}, the grids that we placed over the probe entrance attenuated the plasma density too much allow for collection of microamperes. This resulted in a higher uncertainty in the accuracy of the measurements

We also had problems with RF radiation coming from the helicon power supply. The RF radiation caused the Keithley 2410 source meter and the Keithley 6485 picoammeter to fluctuate from the actual measured/output values. In order to alleviate this problem we placed inductor filters on the input lines for the source meter and the picoammeter, and we surrounded the helicon antenna and magnets in copper mesh shielding. This resulted in fewer fluctuations in the Keithleys; however, the helicon plasma became unstable at higher power settings. Therefore, we

only operated the helicon at 500 watts, 750 watts, and 1000 watts. Furthermore, the signal fluctuations at 13.56 MHz, in addition to the low collected current resulted in low signal to noise ratios and thus, uncertainties in the data.

Despite these issues, a clear drop in the collected current can be seen in the current vs. voltage sweeps along with a peak in the IEDF characteristics. Since the expected ion energy in a helicon discharge is lower than that of the ion source, we ran voltage sweeps only from 0 V to 150 V. In addition, we wanted to investigate the effect of the electron-repelling grid on the measured IEDF, so for both analyzers, we measured data at various electron-repelling grid potentials: 0 V, -30 V, -60 V, and -100 V. We also ran the MRPA at three different electron-suppression grid potentials (0 V, -5.7 V, and -11.3 V) to determine any effects from that grid.

1. Micro Retarding Potential Analyzer

Overall, we found that the most probable ion voltage measured with the MRPA was between 17 V and 40 V at two downstream locations (-25.5 cm and -51.5 cm) while operating the helicon at 500 W and maximum magnetic field strength (415 G). In general, we measured the higher ion energies further downstream. Also, we found that as we increased the magnitude of the potential on the electron-repelling grid from 0 V to -100 V, the most probable ion voltage decreased. Similarly, when the magnitude of the potential on the electron-suppression grid increases from 0

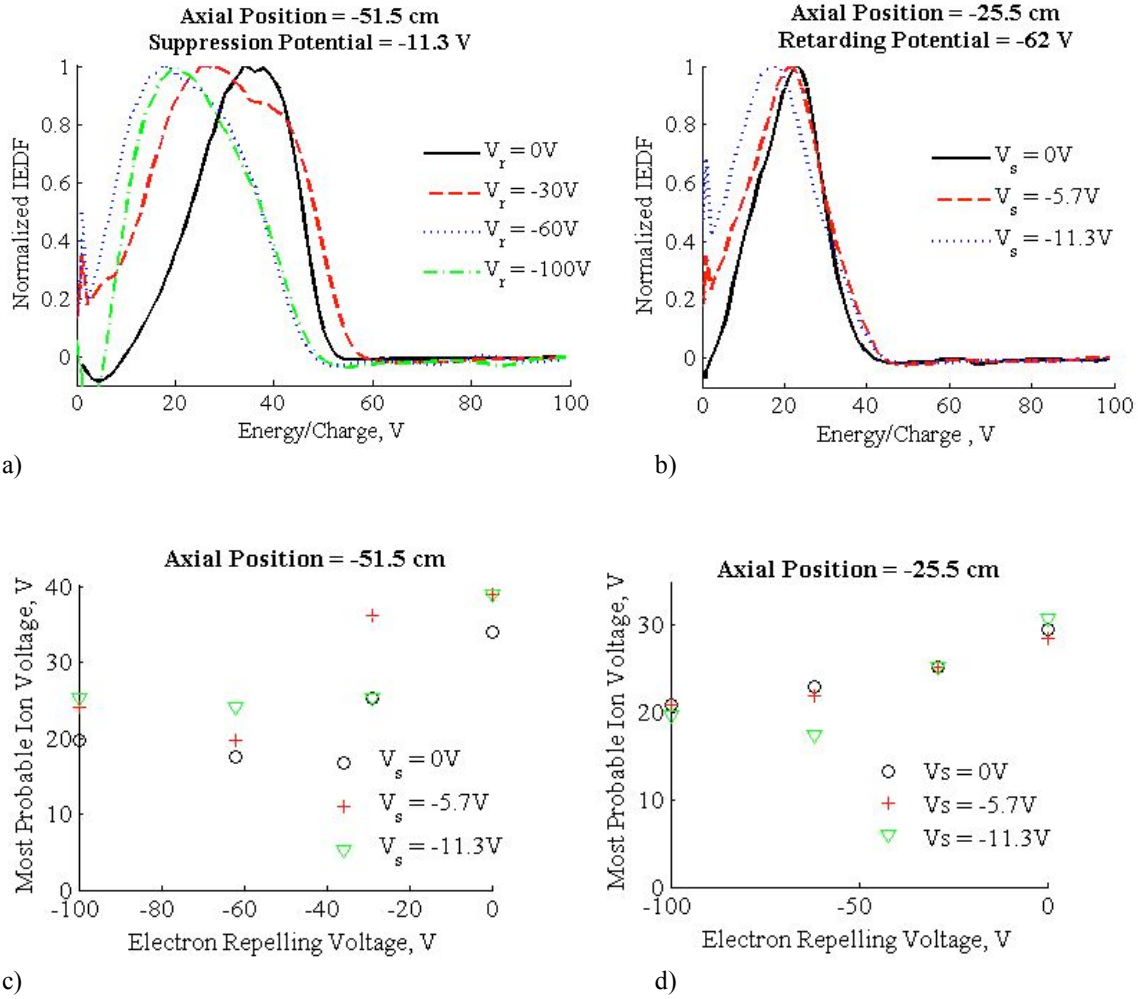

Figure 9. IEDF characteristics and most probable voltage results from MRPA. *All data was taken with the helicon operating at 500 W total power and a peak magnetic field strength of 415 G. Figure 9a shows the normalized IEDFs vs. electron-repelling grid potential for a fixed electron-suppression potential. Figure 9b is the normalized IEDFs vs. electron-suppression grid potential for a fixed electron-repelling potential. Figures 9c and 9d are the most probable ion voltages as a function of the electron-repelling and suppression voltages for two different positions.*

V to -11.3 V, the most probable ion voltage decreases slightly. This is unexpected since one would think the negative potential of the repelling and suppression grids would accelerate the ions. Figure 9 illustrates the change in V_{mp} as a function of repelling and suppression voltage for two different downstream positions. The initial jump that occurs at 0 V is a result of the Keithley 2410 source meter, and not a characteristic of the plasma.

Also illustrated in Fig. 9 is an increase in ion energy further downstream of the helicon source. The ions at 51.5 cm downstream of the helicon have about 5 V to 10 V more energy than those only 25.5 cm downstream. This type of behavior has been seen before in helicon sources and is usually associated with the presence of a double layer.[9]

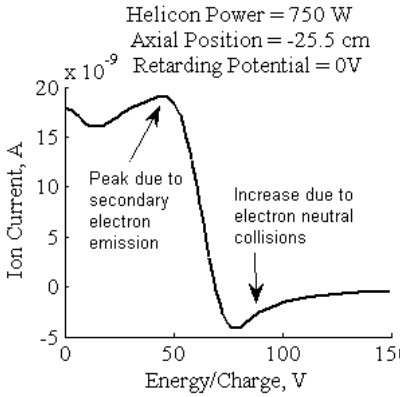

Figure 10. Current vs. voltage sweep. *Performed on SRPA (no suppression grid) with no retarding potential.*

2. Slit Retarding Potential Analyzer

Data measured from the SRPA shows very clearly the need for an electron-suppression grid/slit. Without one, the secondary electrons emitted by collisions with the collector are free to oscillate along the analyzer axis. This causes a slight increase in the collected current around the region of zero ion energy.[10] Data from the SRPA also demonstrates the need for a sufficient negative potential to be applied to the electron-repelling slit. When the retarding potential becomes larger than the maximum ion kinetic energy, the collected current should go to zero. However, in the absence of an applied potential on the electron-repelling slit, or when that potential is insufficient, ionization occurs in the analyzer caused by electron-neutral collisions. This results in a parasitic current flowing into the collector at higher retarding energies.[10] Both of these phenomena are shown in Fig. 10.

The most probable ion voltage measured by the SRPA is higher than that measured by the MRPA by a factor of about three, ranging from 55 V to 100 V. One reason for this could be that the collector was measuring the current with respect to facility ground instead being isolated, as was expected.[11] This was possible if a short occurred between the shielding on the BNC cable and the facility ground. For this new condition, the true ion voltage would be equal to the plasma potential subtracted from the measured ion voltage.

Another difference that we found when comparing the measured data from the MRPA and the SRPA is that when we increased the magnitude of the potential applied to the electron-repelling slit on the SRPA, the most probable ion voltage increased. This situation is opposite to what we measured with the MRPA, but the SRPA case is more expected. A strong negative potential applied to the electron-repelling slit could cause the ions to accelerate.

As is the case with the MRPA, we found that the most probable ion energy is higher further downstream of the helicon source exit. Furthermore, we found that increasing the total RF power into the helicon source resulted in an increase in the most probable ion energy. This increase is a function of the retarding potential. As the retarding potential goes from 0 V to -100 V, the effect of the input power on the ion energy increases. Figure 11 shows this graphically and also contains plots of data obtained from measurements done with the SRPA downstream of the helicon source at two axial locations, two total RF power settings and four electron-repelling potentials.

V. Conclusion

Two retarding potential analyzers were designed, built, and tested on a helicon source at PEPL. Before testing on the helicon source, they were calibrated in the monoenergetic beam of a 3-cm-diameter commercially purchased ion source. Although the signal to noise ratio of these calibrations was low, a peak in the IEDF could still be discerned. Both the MRPA and the SRPA gave similar ion energies that were lower than what we expected, but the difference can be explained. Testing of the RPAs in the plume of the PEPL helicon source gave differing results between the two analyzers. Possible explanations for the discrepancies were discussed. Despite the difficulties that arose, both RPAs functioned and measured a most probable ion energy. Future work to improve the reliability of the RPAs should involve further calibrations using the ion source and additional tests on the helicon source with the attenuation grids on the front of the analyzers removed. This will allow for greater particle flux, and therefore, greater signal to noise ratio. In addition, work should be done to reduce the affect that RF radiation plays in the measured ion energy data. Finally, an electron-suppression slit should be added to the SRPA, and the slit width should be made adjustable.

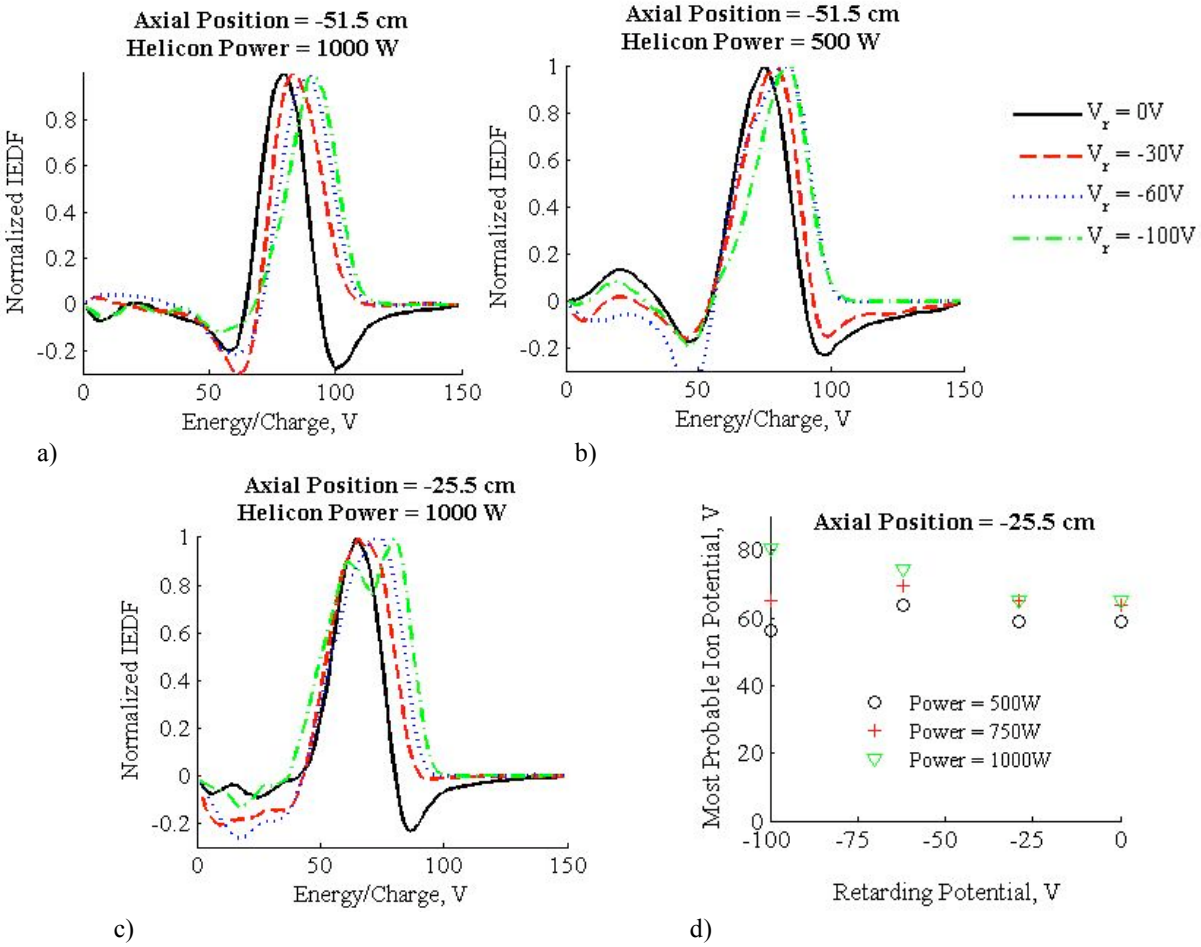

Figure 11. IEDF characteristics and most probable voltage results from SRPA. *All data was taken with the helicon operating at maximum magnetic field strength (peak = 415 G). Figures 11a – 11c are normalized IEDF characteristics for various total helicon RF power, axial positions and retarding potential. Figure 11d is a plot of the most probable ion voltage as a function of the retarding potential and the total helicon RF power.*

Acknowledgments

The authors would like to thank the Michigan Space Grant Consortium and ElectroDynamic Applications Inc. for their support of this work. In addition, Fig. 3b was drawn by an undergraduate student in the mechanical engineering department at the University of Michigan, Mike Rayle. Finally, support from our department technicians, Tom Griffin and Dave McClean is greatly appreciated.

References

[1]Grantham, W. L., "Flight Results of a 25 000-foot-per-second Reentry Experiment using Microwave Reflectometers to Measure Plasma Electron Density and Standoff Distance," NASA Technical Note D-6062, 1970.

[2]Jones, W. L., Jr., and Cross, A. E., "Electrostatic Probe Measurements of Plasma Parameters for Two Reentry Flight Experiments at 25 000 feet-per-second," NASA Technical Note D-6617, 1972.

[3]Hutchinson, I. H., *Principles of Plasma Diagnostics, Second Edition*, Cambridge University Press, Cambridge, UK, 2002.

[4]Beal, B. E., Gallimore, A. D., Morris, D. P., Davis, C., and Lemmer, K. M., "Development of an Annular Helicon Source for Electric Propulsion Applications," AIAA 2006-4841, 42nd Joint Propulsion Conference, Sacramento, CA, July 2006.

[5]Chen, F. F., "Experiments on Helicon Plasma Sources," *Journal of Vacuum Science and Technology A,* Vol. 10, No. 4, July-Aug., 1992.

[6]Conway, G. D., Perry, A. J., and Boswell, R. W., "Evolution of Ion and Electron Energy Distributions in Pulsed Helicon Plasma Discharges," *Plasma Sources Science and Technology*, Vol. 7, 1998, pp. 337-347

[7]Smith, T. B., Ngom, B. B., Linnell, J. A., and Gallimore, A. D., "Diode Laser-Induced Fluorescence of Xenon Ion Velocity Distribution Functions," AIAA-2005-4406, 41st Joint Propulsion Conference, Tucson, AZ, July 2005.

[8]Beal, B. E., and Gallimore, A. D., "Energy Analysis of a Hall Thruster Cluster," IEPC-2003-035, 28th International Electric Propulsion Conference, Toulouse, France, March 2003.

[9]Sun, X., Keesee, A. M., Costel, B., and Scime, E., "Observations of Ion-Beam Formation in a Current-Free Double Layer, *Physical Review Letters*, Vol. 95, No. 2, July 2005.

[10]Bohm, C., and Perrin, J., "Retarding-Field Analyzer for Measurements of Ion Energy Distributions and Secondary Electron Emission Coefficients in Low-Pressure Radio Frequency Discharges," *Review of Scientific Instruments*, Vol. 64, No. 1, January 1993.

[11]Hofer, R. R., Haas, J. M., and Gallimore, A. D., "Ion Voltage Diagnostics in the Far-Field Plume of a High-Specific Impulse Hall Thruster," AIAA-2003-4556, 39th Joint Propulsion Conference, Huntsville, AL, July 2003.